applied sciences

MDPI

Article

Calibration of Mean Wind Profiles Using Wind Lidar Measurements

Vincenzo Sepe [1], Alberto Maria Avossa [2,*], Fabio Rizzo [3] and Francesco Ricciardelli [2]

[1] Department of Engineering and Geology, University "G. d'Annunzio" of Chieti-Pescara, 65127 Pescara, Italy; vsepe@unich.it
[2] Department of Engineering, University of Campania "Luigi Vanvitelli", 81031 Aversa, Italy; friccia@unicampania.it
[3] Department of Architecture, Construction and Design, Politechnic University of Bari, 70125 Bari, Italy; fabio.rizzo@poliba.it
* Correspondence: albertomaria.avossa@unicampania.it; Tel.: +39-081-501-0304

Abstract: This paper explores the applicability of Lidar wind measurements for the calibration of mean wind profiles depending on the extension in time and space of the available measurements. Starting from logarithmic wind speed profiles corresponding to different site conditions, pseudo-experimental wind speed profiles are generated artificially by adding a zero-mean Gaussian-distributed noise, representative of realistic measurement errors. Then, a least-square fitting procedure is applied to identify the roughness length and the zero-plane displacement. The results obtained show an increase in the scatter of the estimated parameters of the logarithmic law with increasing elevation of the lowest measurement point. Then, a parametric study is developed to analyse the influence of the number of available experimental profiles on the uncertainty associated with the estimated logarithmic law parameters. Based on the results obtained, it can be pointed out that the availability of measurements at low elevations is essential to identify the logarithmic mean wind profile using a reasonable number of observations.

Keywords: Wind Lidar; mean wind profile; wind models

Citation: Sepe, V.; Avossa, A.M.; Rizzo, F.; Ricciardelli, F. Calibration of Mean Wind Profiles Using Wind Lidar Measurements. *Appl. Sci.* **2023**, *13*, 5077. https://doi.org/10.3390/app13085077

Academic Editor: Wei Huang

Received: 24 March 2023
Revised: 12 April 2023
Accepted: 13 April 2023
Published: 18 April 2023

1. Introduction

An accurate representation of winds in the Atmospheric Boundary Layer (ABL) is of great interest to engineers, both to evaluate wind loading on structures and to assess expected wind energy production.

In a neutral surface layer, the wind speed profile can be usefully defined according to different analytical models including Power Law, Logarithmic Law and the Deaves and Harris model [1–4]. Both the Logarithmic Law and the Deaves and Harris model are based on the definition of a roughness length z_0. Moreover, it is widely accepted that, in the urban environment, any analytical law for the mean wind speed profile has to include, as a starting point for the elevation coordinate, a zero-plane displacement z_d, i.e., the level below which the flow is nearly blocked by the obstructing buildings.

Although the values of these parameters are mainly related to surface morphology, their estimation remains difficult. This particularly occurs in urban areas where the marked variability in heights and density of roughness elements produces a complex surface morphology. In this context, few tall buildings often rise above mid-rise buildings or low-rise buildings, whilst in suburbs more homogeneous values of height and density of roughness elements are common.

Generally, the methods used to assess the values of z_0 and z_d can be classified in three types: (i) *reference-based*, (ii) *morphometric* (or *geometric*) and (iii) *anemometric* (or *micrometereological*). Methods of the first type are based on the comparison of a neighbourhood plan and site photography with figures or reference tables available in the literature, e.g., [5–8].

Methods of the second type consist of relating aerodynamic parameters to measures of surface morphometry in terms of the plan area index, e.g., [9]. The last methods use field observations of wind or turbulence to solve for aerodynamic parameters included in theoretical relationships, e.g., those derived from the logarithmic wind profile [10,11].

Within the *anemometric* methods, measurement of the wind velocity field at a given site is essential for defining and validating analytical and numerical models for wind actions on structures. In the last decades, observations of wind speed profiles through Doppler Lidar anemometry have become popular [12–18] despite the inaccuracies associated with non-synchronous measurement and space averaging. Lidars allow a relatively easy acquisition of wind velocities at different heights in a range of several hundred meters above the ground.

On the other hand, it is difficult or impossible to measure through Lidars the wind speed close to the ground. Depending on the characteristics of this device, in fact, the wind velocity can be measured only at points whose distance from Lidar is larger than a given threshold, usually around 30 m. As a matter of fact, the variation of the mean wind speed is more pronounced near the ground; therefore, calibration of the parameters that characterize analytical models is deeply influenced by wind speed values at low elevations, and this may be particularly important in urban areas where the wind flow near the ground interacts with the built environment.

Within this topic, this paper explores to which extent Wind Lidars can be used to calibrate mean wind profiles depending on the available measurements; it is a part of a wider research on the effectiveness of the Lidar methodology for the experimental characterization of wind fields [19]. Numerical analyses are developed to investigate how the identification of the roughness length z_0 and zero-plane displacement z_d is affected by the extension in time and space of the available measurements.

To this end, and with no loss of generality, the logarithmic law has been assumed as representative of the mean wind speed profile, assuming a synoptic wind regime; for different values of z_0 and z_d, a set of profiles of 10-min averaged wind speeds are simulated for moderately strong winds, affected by numerical noise in the typical range of the accuracy of Lidar measurements. The pseudo-experimental wind speed profiles are then assumed as input data for a least-square fitting procedure that allows identification of the parameters z_0 and z_d of the logarithmic profile.

Starting from different morphometric situations, the identified values of z_0 and z_d are discussed in relationship to the number of measuring points and to the height of the lowest available measuring point. As a main result, it can be pointed out that measurements at lower elevations than those provided by Lidars are required to identify the logarithmic profile properly, especially when mean wind speeds close to the ground are of interest.

2. Methodology

As known, the logarithmic law can be assumed as a possible analytic model to describe the mean wind profile during thermally neutral conditions up to 200 m of elevation [20–22]. Matching the law of the wall with the velocity defect law in the inertial sublayer (ISL) [4], and considering the vertical displacement due to the surface obstacles, such as buildings or vegetations, the wind speed profile is given by:

$$u(z) = \frac{u^*}{\kappa} \ln\left(\frac{z - z_d}{z_0}\right) \tag{1}$$

where u^* is the surface friction velocity; $\kappa = 0.4$ is the von Karman constant [23]; z_0 is the surface roughness length; and z_d is the zero plane displacement. The logarithmic law can be also described by the following equation:

$$u(z) = u_{ref} \ln[(z - z_d)/z_0] / \ln\left[\left(z_{ref} - z_d\right)/z_0\right] \tag{2}$$

where u_{ref} is the wind speed at the reference elevation z_{ref}, assumed as the elevation of the lowest measurement point; the wind speed takes the value $u = 0$ at the elevation $z_d + z_0$ above the ground. In the urban environment, it is important to incorporate the displacement height z_d since this is equivalent to set a base for the logarithmic wind profile that considers the physical bulk of the urban canopy. It corresponds to shifting the ground level upwards where the mean momentum sink for the flow is located.

Selection of heights at which to carry out wind measurements in urban areas is a challenge. According to the WMO-*No.8* Guide [24], in densely built-up areas, it can be assumed that the roughness sublayer, in which the effects of individual roughness elements persist, extends to a height of about 1.5 times the mean height of the roughness elements, z_h. Moreover, it is well known from wind tunnel tests and field observations that flow over isolated solid obstacles, e.g., tall buildings, is highly perturbed both immediately over and around it. Consequently, in these cases, it was proposed to place the anemometers at a height larger than the maximum horizontal dimension of the major canopy [25].

This involves, at first, the use of an expensive mast system, which is often not simple to install. As an alternative, the use of Wind Lidars allows acquisition of wind velocities at different heights in a range of a few hundred meters above the ground. These anemometers are based on the principle of an optical Doppler shift between the reference laser beam and the radiation backscattered by aerosols. Due to the high aerosol concentration in urban environments, Lidar measurements can be considered suitable to assess wind profiles in urban areas. In this context, Lidar measurements present some advantages, including the large scan volume, mobility, wind measurements in 3-dimensions, as well as its relatively higher temporal and spatial resolution compared with other measurement devices.

Since Lidar only measures radial velocities, some assumptions on the stationarity of the wind velocity field in time and space are required to derive three velocity components from Lidar data. As a consequence, some uncertainties of measurements especially over complex terrain can arise when the homogeneous assumption used in derived methods is violated. These inherent uncertainties are mainly influenced by errors in identifying sensing distance and elevation angle [26]. Moreover, environmental conditions, such as turbulence intensity and precipitation, introduce additional uncertainties in wind measurements [27]. Consequently, it is expected that future development of the Doppler Lidar technique and data processing algorithms will provide ever more accurate measurements with high spatial and temporal resolutions under different environmental conditions. Despite these uncertainties, Lidar measurements can be considered as a reliable alternative in the assessment of the mean wind profile in urban areas especially in neutral conditions.

To explore to what extent Wind Lidars can be used to calibrate mean wind profiles, four scenarios are selected corresponding to different pairs of nominal parameters z_0 and z_d, representative of different site conditions, as reported in Table 1 and Figure 1. In particular, the four scenarios are defined as such to represent the boundaries of a realistic range of variation of the pair of parameters z_0 and z_d. Case (a) is representative of an urban area densely covered by low-rise buildings of uniform height. Case (b) is representative of a quite densely built-up area with low-rise buildings having rather heterogeneous height. Case (c) is representative of a densely built-up area with medium-rise buildings of uniform height. Case (d) is representative of a densely built-up area with medium-rise buildings having rather heterogeneous height.

Table 1. Pairs of z_0 and z_d parameters used in the simulations.

Case	z_0 [m]	z_d [m]
a	0.05	5
b	1.50	5
c	0.05	20
d	1.50	20

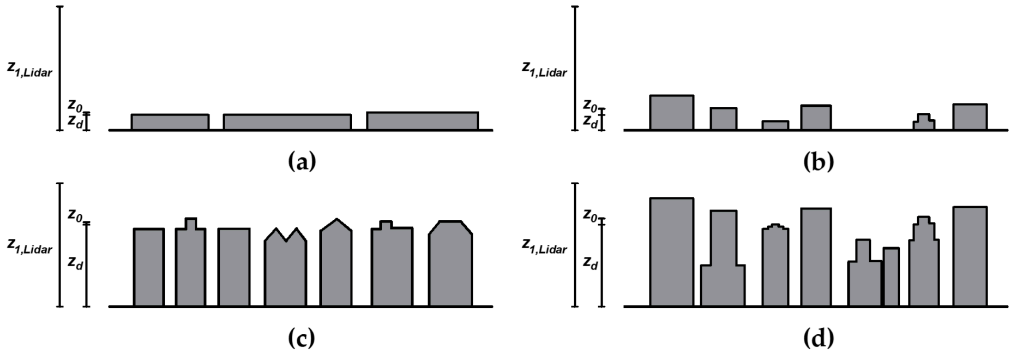

Figure 1. Sketches of roughness configurations of Table 1: Case (**a**) z_0 = 0.05 m, z_d = 5 m; Case (**b**) z_0 = 1.5 m, z_d = 5 m; Case (**c**) z_0 = 0.05 m, z_d = 20 m; Case (**d**) z_0 = 1.5 m, z_d = 20 m. (Adapted from WMO-*No.8* Guide [24]). $z_{1,Lidar}$ is the elevation of the lowest measurement point of Lidar (at 30 m).

For each sample case, a set of 10,000 pseudo-experimental profiles was generated by adding to the ideal (or "exact") logarithmic profile a zero-mean Gaussian noise, characterized at each elevation by a standard deviation equal to 2% of the logarithmic wind speed at that elevation, as representative of realistic measurement errors. The amount of noise added to the profiles was chosen based on the measure error of available Wind Lidars.

For each pseudo-experimental profile, the parameters z_0 and z_d were identified by means of a least-square error minimization procedure, as follows. Identification of the logarithmic law parameters was first performed by assuming that only Lidar measurements are available, with the lowest measurement point at 30 m above the ground; results are discussed in Section 3. As a first step, identification of the optimum value of the friction velocity u^* can be performed solving a three parameters (u^*, z_0 and z_d) optimization problem applied to the median profile of a set of Wind Lidar profiles measured for a given wind sector. Then, each profile measured in that sector can be scaled to the identified value of u^* and considered as a sample profile. Finally, calibration of the optimum pairs of values z_0 and z_d can be performed on the set of scaled measured profiles. In this study, pseudo-experimental profiles were generated by adding a zero-mean Gaussian noise to the same parent logarithmic profile with a given u^*, and each of them can be assumed as a single measured profile already scaled to the value u^*. For each scaled profile, the parameters z_0 and z_d are identified as those minimizing the least-square error between the vector of values $\bar{u}_i$ of the scaled wind speed at the n available elevations z_i and their logarithmic counterpart $(1/\kappa)ln[(z_i - z_d)/z_0]$. Then, the mean values and the coefficients of variation of the pairs of values z_0 and z_d identified for different sets of pseudo-experimental profiles are calculated and discussed.

Different combinations and elevations of the Lidar measurement points will be analysed and discussed in Section 4.1. Finally, the availability of a further point at a lower elevation, provided by, e.g., a sonic or a cup anemometer, will be considered and discussed in Section 4.2.

3. Problem Statement

Assuming that only Lidar measurements are available, and according to the technical specifications so far guaranteed by such devices, the lowest measurement point was assumed at 30 m above the ground, and a maximum of 12 measurement points was considered. As a first example, twelve elevations z = 30, 40, 50, 60, 70, 80, 100, 120, 140, 160, 180, 200 m are considered here, denoted as measurement setup #0 in Table 2.

By means of the least-square error minimization procedure described in Section 2, for the set of pseudo-experimental profiles corresponding to the sample cases of Table 1, the parameters z_0 and z_d of the logarithmic law were identified for measurement setup #0.

Table 2. Elevation of measurement points for different setup.

Setup	Elevation of Measurement Points [m]
#0	z = 30, 40, 50, 60, 70, 80, 100, 120, 140, 160, 180, 200
#1	z = 30, 35, 40, 50, 60, 70, 80, 100, 120, 140, 170, 200
#2	z = 30, 35, 40, 45, 50, 60, 70, 80, 110, 140, 170, 200
#3	z = 30, 35, 40, 45, 50, 55, 60, 70, 90, 120, 160, 200
#4	z = 30, 32, 34, 37, 40, 45, 50, 55, 60, 70, 120, 200

The scatter of the identified parameters with respect to the target pair z_0 and z_d used to generate the pseudo-experimental profiles is shown in Figure 2, where the identified parameters of each profile correspond to a green point on the z_0–z_d plane, and a black square indicates their average values, while the red circle indicates their target values.

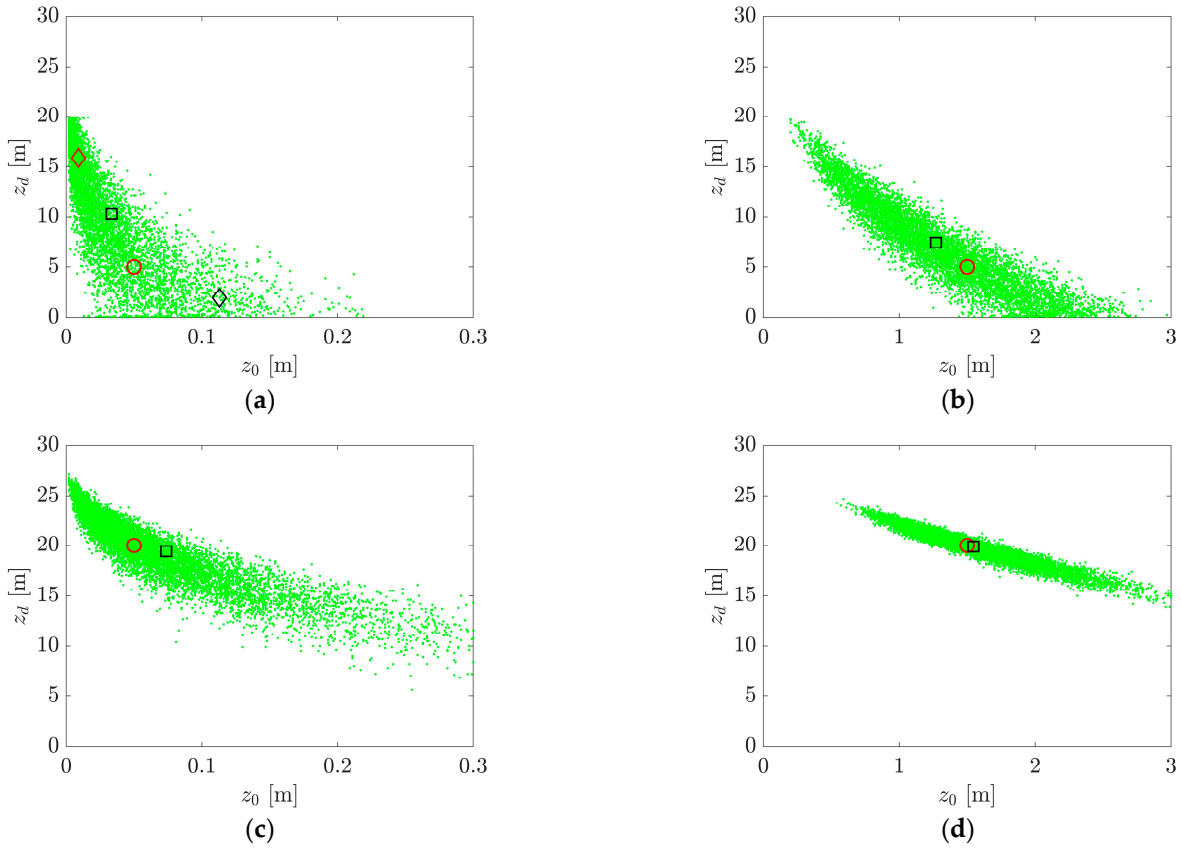

Figure 2. Identified parameters z_0 and z_d (green points) and their average values (black squares), and parent values (red circles) used to generate the pseudo-experimental profiles: Case (**a**) z_0 = 0.05 m, z_d = 5 m; Case (**b**) z_0 = 1.5 m, z_d = 5 m); Case (**c**) z_0 = 0.05 m, z_d = 20 m); Case (**d**) z_0 = 1.5 m, z_d = 20 m). Diamonds in diagram (**a**) indicate the identified pairs z_0 and z_d of profiles represented in Figure 3.

A very large scatter can be observed among the pairs of parameters z_0 and z_d identified from the different pseudo-experimental profiles belonging to the same case. However, their average values (black squares) are quite in agreement with the target values of z_0 and z_d for Case (d), and with the target value of z_d value for Case (c). These two cases correspond to the larger values of z_d. On the other hand, the average values are rather away from the target values for Case (a) and Case (b), corresponding to lower values of z_d. According to these results, the quality of the mean identified parameters very much depends on the elevation of the first available measurement point. This explains the poor identification of the logarithmic law parameters (and in particular the zero-plane displacement z_d) when

the lowest measurement point (at 30 m) is far from the zero-speed elevation $z_0 + z_d$ of the wind profile, as for the Case (a) and Case (b) in Figure 2.

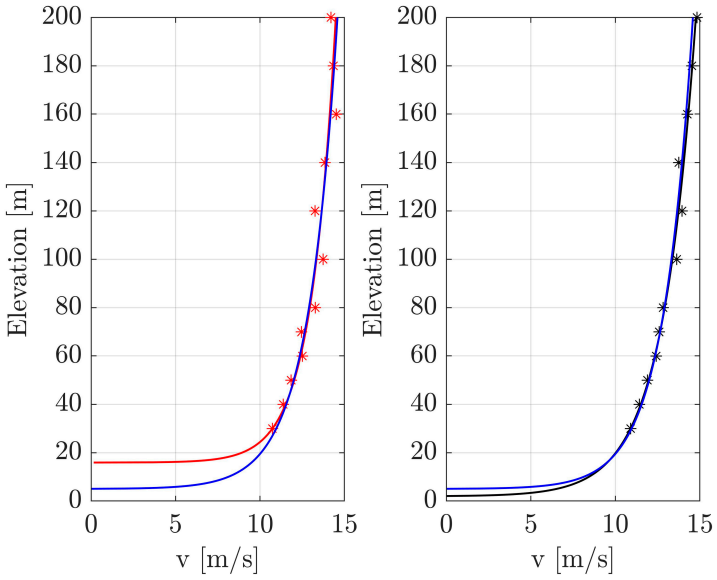

Figure 3. Measurements points (red and black stars) and identified profiles (red and black lines) corresponding to two different pairs of parameters z_0 and z_d (red and black diamonds in Figure 2a), and comparison with the target profile for Case (a) (blue line).

Although the pairs reported in Figure 2 are quite scattered, the corresponding interpolated profiles are very close to each other in the range of measured data, i.e., at elevations above 30 m. On the other hand, the interpolated profiles are very scattered in their extrapolation at lower elevations. Sample of trends are shown in Figure 3 for Case (a) of Table 1; two interpolated profiles derived from two sets of pseudo-experimental points are shown, corresponding to the red and black diamonds in Figure 2a, respectively; they prove to be different from each other and far from the target profile at low elevations. All the profiles are scaled to a velocity value equal to 12 m/s at the elevation of 50 m.

To assess the statistical significance of the ensemble averages μ_{z0} (N) and μ_{zd} (N) of the identified profile parameters for different values of the sample size N, the following procedure is applied. (a) M = 1000 sets of N pseudo-experimental profiles each are selected from the available 10,000; (b) for each of the M = 1000 sets of N profiles, the average parameters μ_{z0} (i) and μ_{zd} (i) were evaluated, i = 1 to 1000, by averaging the parameters $z_0(i,j)$ and $z_d(i,j)$, with j = 1 to N; (c) the mean values, μ_{z0} (N) and μ_{zd} (N), the standard deviation, σ_{z0} (N) and σ_{zd} (N), and the Coefficient of Variation, $CoVz_0(N)$ and $CoVz_d(N)$, of μ_{z0} (i) and μ_{zd} (i) were calculated for each value of N.

In Figures 4 and 5, the bias of the mean values $\mu_{z0}(N)$ and $\mu_{zd}(N)$, together with the confidence interval (bias $\pm$ Coefficient of Variation), is shown as a function of the number N of measured profiles for the 4 cases in Table 1. In particular, the relative bias is defined as the ratio between the mean value and target value of the parameters z_0 and z_d, with a relative bias of one representing an unbiased estimation. These results show how an accurate estimation of the pair of parameters z_0 and z_d can be achieved only for sites with $z_0 + z_d$ values approaching the lowest measurement point (e.g., Case (d)), and when a reasonably large number of measured profiles is available (e.g., $N > 50$). On the other hand, for sites with a larger distance between the base of the logarithmic wind profile and the lowest measurement point (e.g., Case (a) and Case (b)), an accurate estimation of the profile parameters cannot be achieved even when a very large number of measures is available.

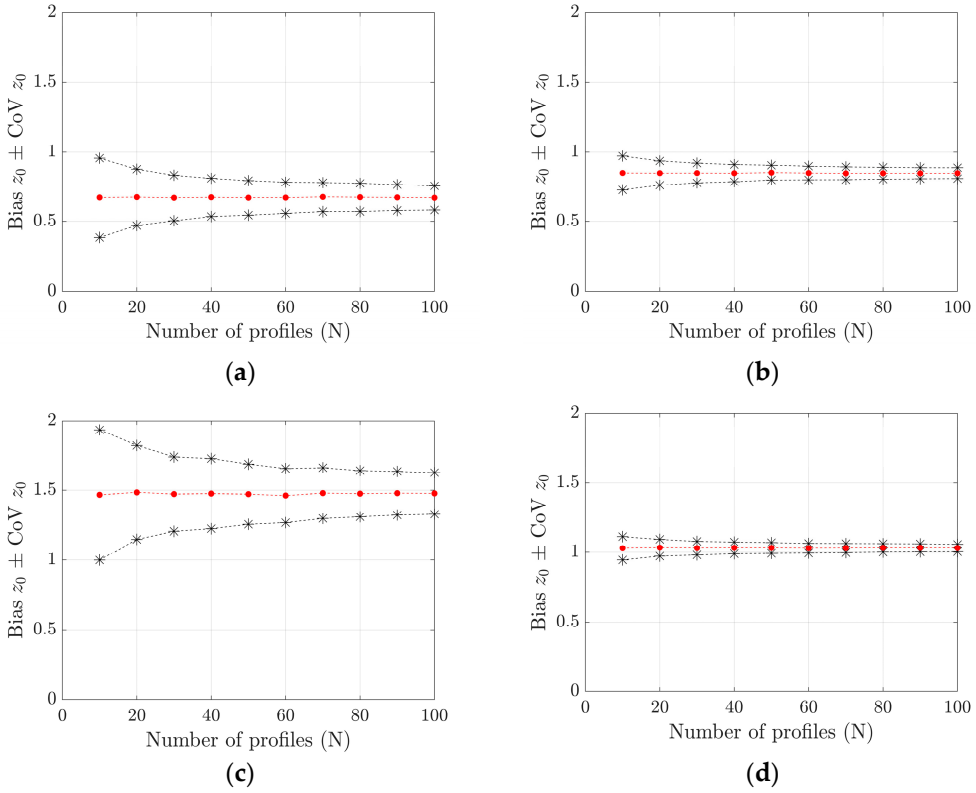

Figure 4. Bias (red circles) and confidence interval (bias ± coefficient of variation, black stars) of z_0 as a function of the sample size N: Case (**a**) z_0 = 0.05 m, z_d = 5 m; Case (**b**) z_0 = 1.5 m, z_d = 5 m; Case (**c**) z_0 = 0.05 m, z_d = 20 m; Case (**d**) z_0 = 1.5 m, z_d = 20 m.

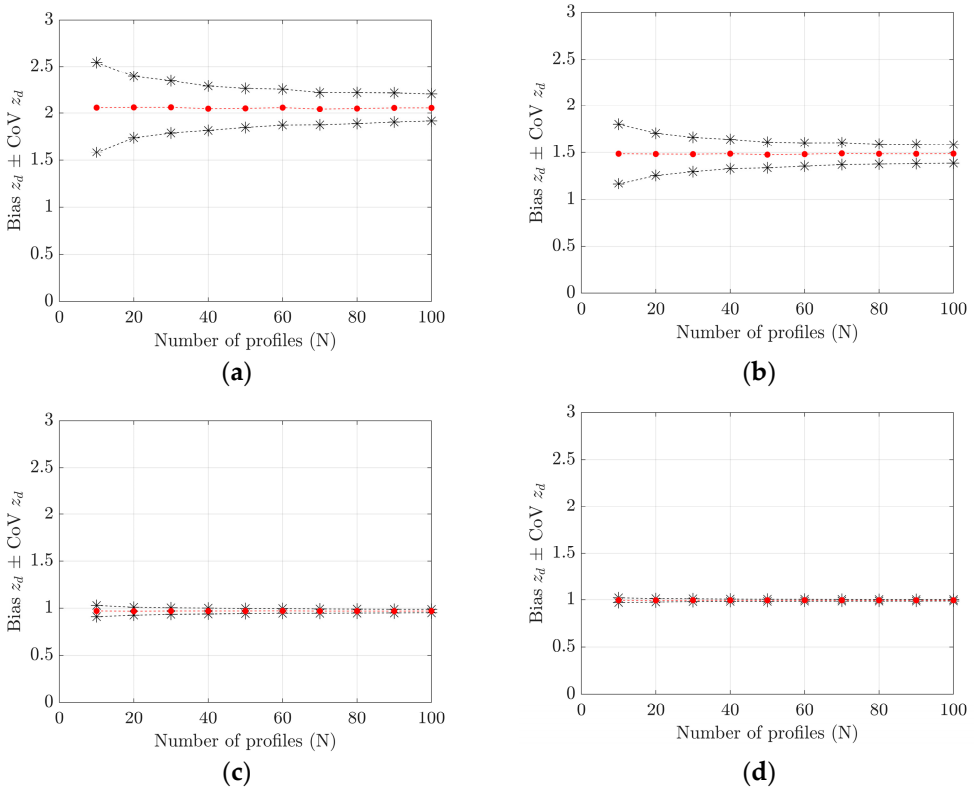

Figure 5. Bias (red circles) and confidence interval (bias ± coefficient of variation, black stars) of z_d as a function of the sample size N: Case (**a**) z_0 = 0.05 m, z_d = 5 m; Case (**b**) z_0 = 1.5 m, z_d = 5 m; Case (**c**) z_0 = 0.05 m, z_d = 20 m; Case (**d**) z_0 = 1.5 m, z_d = 20 m.

4. Results and Discussion

The results presented in Section 3 highlight that, using a commercial Lidar anemometer with 12 measurement points rather uniformly distributed between 30 m and 200 m (Setup #0 in Table 2), a very large scatter is observed among the pairs of parameters z_0 and z_d identified from different measured profiles. Moreover, in cases of sites with a large distance between the elevation $z_0 + z_d$ and the lowest measurement point, an accurate estimation of the profile parameters cannot be achieved.

To improve the accuracy in the estimation of z_0 and z_d, two alternative strategies are investigated. The first is based on a the analysis of different choices of the elevations of the measurement points; if successful, this strategy would enable the use of available Lidars without the need for additional instruments. The second relies on the availability of a further point of measure at a lower elevation than the lowest Lidar point of measure; this would require installation of a sonic or a cup anemometer together with the Lidar.

4.1. Optimization of the Choice of Measurement Elevations

Assuming that the Lidar lowest measurement point is at 30 m above the ground, and a maximum of 12 measurement points is available, four additional scenarios are considered, indicated as setups #1 through #4 in Table 2. The choice of the measurement points in the additional setups is driven by the idea that a larger number of points close to the lowest elevation should bring an improvement in the accuracy of the derivatives of the identified profile, therefore improving the accuracy of its extrapolation to the lower elevations.

In particular, limited to Case (a) in Table 1, the results are presented in Figure 6 in terms of bias and Coefficient of Variation (CoV) within an ensemble of $M = 1000$ cases of the mean values $\mu_{z0}(N)$ and $\mu_{zd}(N)$. These results highlight that the strategy of gathering measurement points close to the lowest point does not lead to any substantial increase in the accuracy of the estimated values of z_0 and z_d. Similar results were obtained for cases (b), (c) and (d) in Table 1, which are not shown here for brevity.

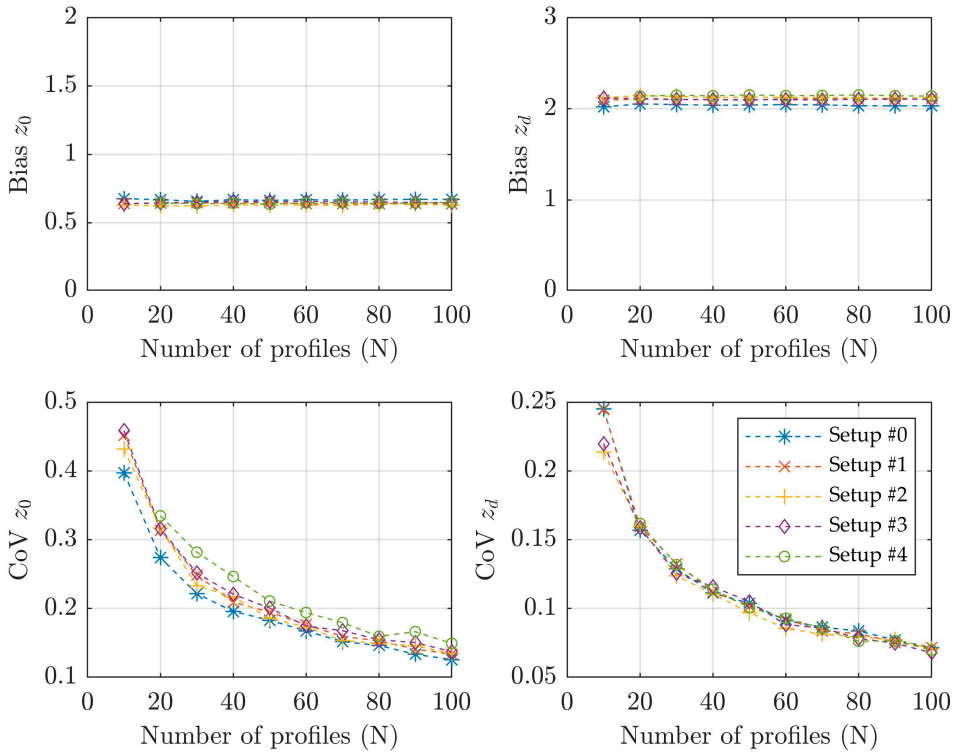

Figure 6. Bias and Coefficient of Variation of μ_{z0} and μ_{zd} as a function of the sample size N of available measured profiles for the different measurement Setups of Table 2: Case (a) $z_0 = 0.05$ m, $z_d = 5$ m.

4.2. Availability of an Additional Point of Measurement at Lower Elevation

Another possible strategy to improve the accuracy of the results is that of adding a further point of measurement at an elevation lower than the lowest point provided by the Lidar. This is accomplished starting from measurement Setup #0 in Table 2 by adding a point of measure at an elevation ζ equal to 0.1, 0.2, 0.4 or 0.7 times the gap between the zero speed elevation ($z_0 + z_d$) and the elevation of the lowest measurement point of Lidar (30 m).

The results are presented in terms of bias and CoV within an ensemble of $M = 1000$ cases of the mean values $\mu_{z0}(N)$ and $\mu_{zd}(N)$ for all the cases reported in Table 1 (Figures 7–10).

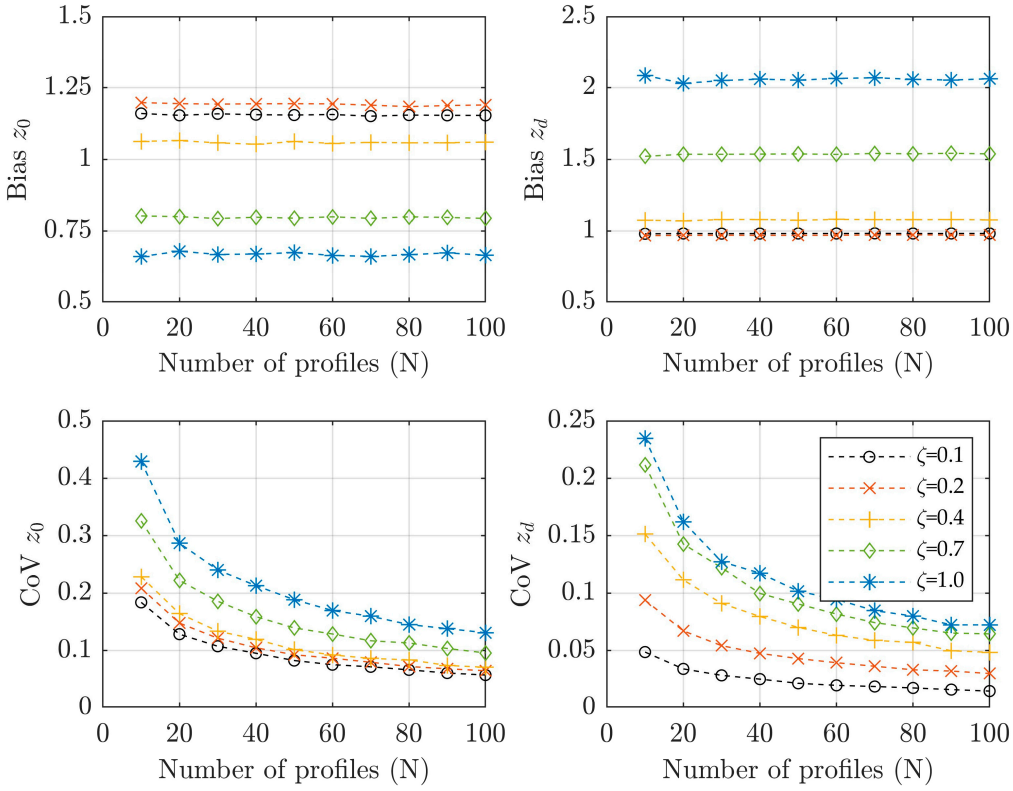

Figure 7. Bias and Coefficient of Variation of μ_{z0} and μ_{zd} as a function of the sample size N of available measured profiles: Case (a) ($z_0 = 0.05$ m, $z_d = 5$ m).

The results highlight that the addition of a lower point of measure allows to eliminate any possible bias existing on the estimate of z_d; however, it reduces but not always eliminates the bias on z_0. In particular, it is noticed that the lower measurement point is unable to eliminate the bias on z_0 for cases (a) and (c) in Table 1, corresponding to a roughness length of 0.05 m. In any case, the bias seems not to be affected by the number of available profiles. On the other hand, in all cases and for both z_0 and z_d, the uncertainty on the estimated parameter reduces when a lower point of measure is added; the CoV of z_d can be reduced to values lower than 2% when $N = 100$ profiles are available, and the CoV of z_0 can be reduced to values lower than 7%.

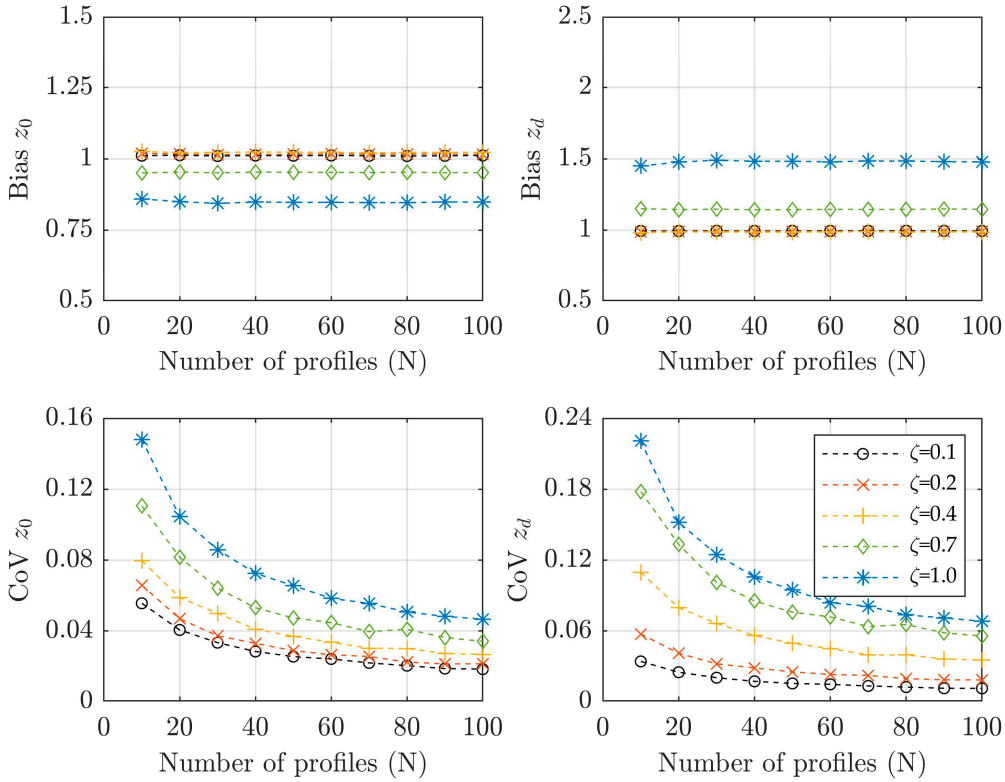

Figure 8. Bias and Coefficient of Variation of μ_{z0} and μ_{zd} as a function of the sample size N of available measured profiles: case (b) (z_0 = 1.5 m, z_d = 5 m).

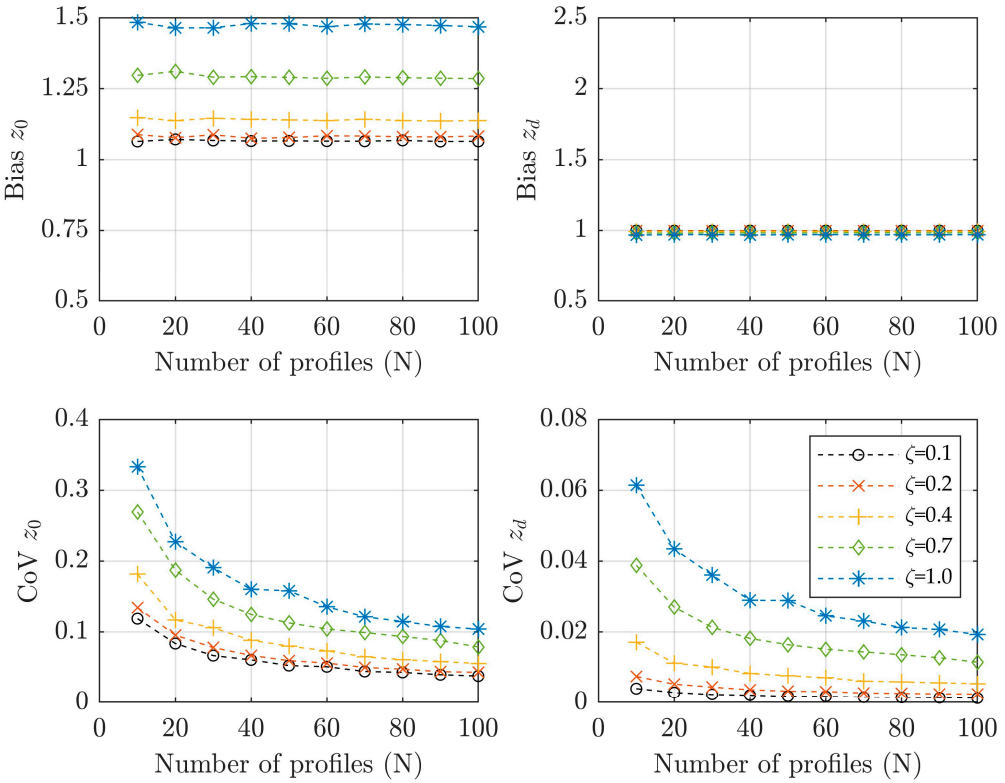

Figure 9. Bias and Coefficient of Variation of μ_{z0} and μ_{zd} as a function of the sample size N of available measured profiles Case (c) (z_0 = 0.05 m, z_d = 20 m).

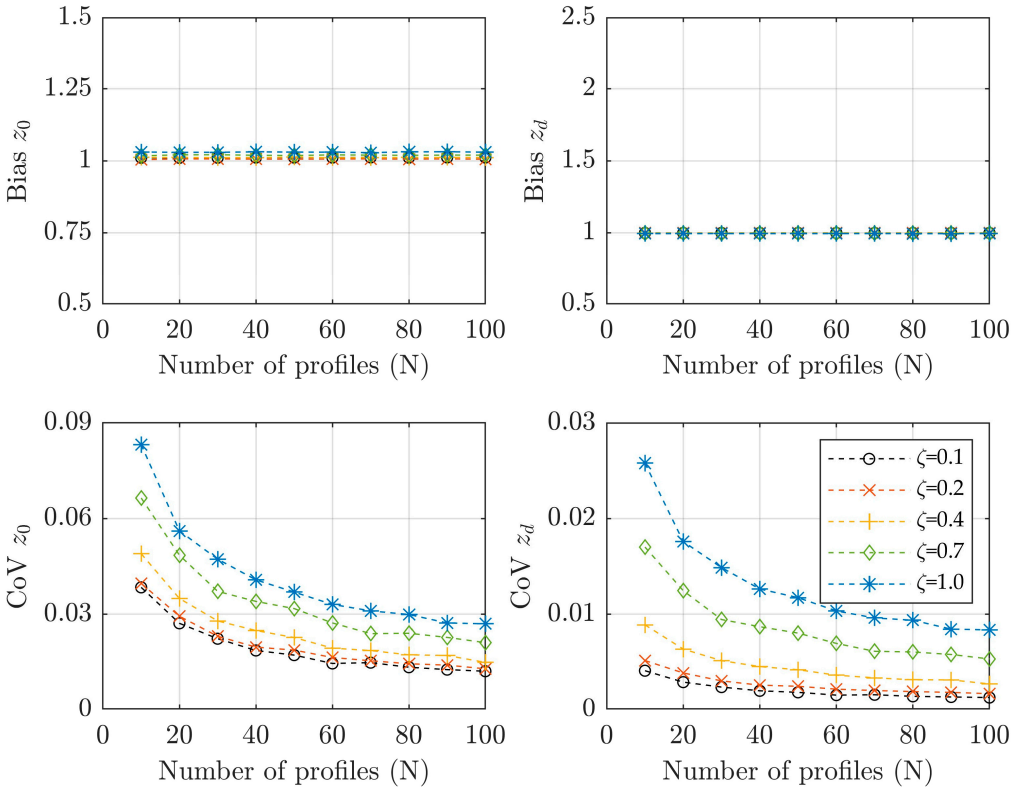

Figure 10. Bias and Coefficient of Variation of μ_{z0} and μ_{zd} as a function of the sample size N of available measured profile: Case (d) (z_0 = 1.5 m, z_d = 20 m).

5. Conclusions

In this paper, pseudo-experimental neutral mean wind profiles were used to investigate the capability of available Wind Lidars at identifying the model parameters of the logarithmic law. It was found that the technical limitation of the lowest possible measurement point at 30 m is a bottleneck for the accuracy of the results; this is particularly the case in open country or suburban exposures where both the roughness length and the zero-plane displacement are low. In fact, not only the scatter of the identified parameters is quite large, but even if a large number of profiles is available, the mean values of the identified parameters do not converge to the exact one; in other words, identification introduces a bias.

To overcome this limitation, two strategies were investigated. The first is that of optimising the choice of the elevations of measure by concentring a large number of them only slightly above 30 m; this choice is expected to bring a better definition of the derivatives of the mean profile at z = 30 m, therefore improving the accuracy of its extrapolation below 30 m. Unfortunately, this expedient proved unsuccessful.

The second strategy is related to the possibility of adding a further measurement point below 30 m, using either a sonic or a cup anemometer; this of course brings extra costs. An additional point of measure definitely improves the reliability of the results but does not necessarily eliminate the bias; as a matter of fact, some bias on z_0 remains even if the extra measurement point is located at a very low elevation.

The results presented are part of a wider research on the quantification and modelling of the uncertainty on wind loads, some of which is associated with the uncertainty on the characteristics of the wind flow in the atmospheric boundary layer. It is concluded that, if properly designed, full scale measurements can be very helpful in reducing such accuracy but do not allow to eliminate it. As an alternative, a combination with other methods, e.g., morphometric methods, could be of help.

Author Contributions: Conceptualization, A.M.A., V.S., F.R. (Fabio Rizzo) and F.R. (Francesco Ricciardelli); methodology, A.M.A., V.S., F.R. (Fabio Rizzo) and F.R. (Francesco Ricciardelli); software, A.M.A., V.S., F.R. (Fabio Rizzo) and F.R. (Francesco Ricciardelli); validation, A.M.A., V.S., F.R. (Fabio Rizzo) and F.R. (Francesco Ricciardelli); writing—original draft preparation, A.M.A., V.S., F.R. (Fabio Rizzo) and F.R. (Francesco Ricciardelli); writing—review and editing, A.M.A., V.S., F.R. (Fabio Rizzo). and F.R. (Francesco Ricciardelli); supervision, A.M.A., V.S., F.R. (Fabio Rizzo) and F.R. (Francesco Ricciardelli). All authors have read and agreed to the published version of the manuscript.

Funding: This research received no external funding.

Data Availability Statement: Not applicable.

Conflicts of Interest: The authors declare no conflict of interest.

Abbreviations

List of abbreviations and symbols.

ABL	Atmospheric boundary layer
ISL	Inertial sublayer
N	number of profile samples in a set
M	number of sets of pseudo-experimental profiles
κ	von Karman constant
n	number of available elevations
u^*	surface friction velocity
$u(z)$	wind speed profile
z	elevation
z_d	zero-plane displacement
z_h	mean height of roughness elements
z_{ref}	reference elevation
z_0	roughness length
$z_{1,Lidar}$	elevation of the lowest measurement point of Lidar
$\mathrm{CoV}_{zd}(N)$	ensemble coefficient of variation of z_d
$\mathrm{CoV}_{z0}(N)$	ensemble coefficient of variation of z_0
$\mu_{zd}\ (N)$	ensemble average of z_d
$\mu_{z0}\ (N)$	ensemble average of z_0
$\sigma_{zd}\ (N)$	ensemble standard deviation of z_d
$\sigma_{zd}\ (N)$	ensemble standard deviation of z_0

References

1. Davenport, A.G. Rationale for determining design wind velocities. *J. Struct. Eng.* **1960**, *86*, 39–68. [CrossRef]
2. Blackadar, A.K.; Tennekes, H. Asymptotic similarity in neutral barotropic planetary boundary layers. *J. Atmos. Sci.* **1968**, *25*, 10151020. [CrossRef]
3. Deaves, D.; Harris, R. *A Mathematical Model of the Structure of Strong Winds*; Report 76; Construction Industry Research and Information Association: London, UK, 1978.
4. Simiu, E.; Scanlan, R. *Wind Effects on Structures—Fundamentals and Applications to Design*; John Wiley and Sons Inc.: Hoboken, NJ, USA, 1996.
5. Grimmond, C.S.B.; Oke, T.R. Aerodynamic properties of urban areas derived from analysis of surface form. *J. Appl. Meteorol. Climatol.* **1999**, *38*, 1262–1292. [CrossRef]
6. Wieringa, J.; Davenport, A.J.; Grimmond, C.S.B.; Oke, T.R. New revision of Davenport roughness classification. In Proceedings of the 3EACWE, Eindhoven, The Netherlands, 2–6 July 2001.
7. Steward, I.D.; Oke, T.R. Local climate zones for urban temperature studies. *J. Bull. Am. Meteorol. Soc.* **2012**, *93*, 1879–1900. [CrossRef]
8. Yu, J.; Stathopoulos, T.; Li, M. Estimating Exposure Roughness Based on Google Earth. *J. Wind Eng. Ind. Aerodyn.* **2021**, *147*, 04020353. [CrossRef]
9. Macdonald, R.W.; Griffiths, R.F.; Hall, D.J. An improved method for the estimation of surface roughness of obstacle arrays. *Atmos. Environ.* **1998**, *32*, 1857–1864. [CrossRef]
10. Schaudt, K. A new method for estimating roughness parameters and evaluating the quality of observations. *J. Appl. Meteorol.* **1998**, *37*, 470–476. [CrossRef]

11. Martano, P. Estimation of surface roughness length and displacement height from single-level sonic anemometer data. *J. Appl. Meteorol.* **2000**, *39*, 708–715. [CrossRef]
12. Drew, D.R.; Barlow, J.F.; Lane, S.E. Observations of wind speed profiles over Greater London, UK, using a Doppler lidar. *J. Wind Eng. Ind. Aerodyn.* **2013**, *121*, 98–105. [CrossRef]
13. Lane, S.E.; Barlow, J.F.; Wood, C.R. An assessment of a three-beam doppler lidar wind profiling method for use in urban areas. *J. Wind Eng. Ind. Aerodyn.* **2013**, *119*, 53–59. [CrossRef]
14. Wood, C.R.; Pauscher, L.; Ward, H.; Kotthaus, S.; Barlow, J.; Gouvea, M.; Lane, S.; Grimmond, C.S.B. Wind observations above an urban river using a new lidar technique, scintillometry and anemometry. *Sci. Total Environ.* **2013**, *442*, 527–533. [CrossRef] [PubMed]
15. Lim, K.E.W.; Watkins, S.; Clothier, R.; Ladani, R.; Mohamed, A.; Palmer, J.L. Full-scale flow measurement on a tall building with a continuous-wave Doppler Lidar anemometer. *J. Wind Eng. Ind. Aerodyn.* **2016**, *154*, 69–75. [CrossRef]
16. Demartino, C.; Avossa, A.M.; Ricciardelli, F.; Calidonna, C.R. Wind profiles identification using wind LIDARS: An application to the area of Lametia Terme. In Proceedings of the 7th European and African Conference on Wind Engineering, EACWE, Liège, Belgium, 4–7 July 2017.
17. Kent, C.W.; Grimmond, C.S.B.; Gatey, D.; Burlow, J.F. Assessing methods to extrapolate the vertical wind-speed profile from surface observations in a city centre during strong winds. *J. Wind Eng. Ind. Aerodyn.* **2018**, *173*, 100–111. [CrossRef]
18. Ricciardelli, F.; Pirozzi, S.; Mandara, A.; Avossa, A.M. Accuracy of mean wind climate predicted from historical data through wind LIDAR measurements. *Eng. Struct.* **2019**, *201*, 109771. [CrossRef]
19. Sepe, V.; Rizzo, F.; Ricciardelli, F.; Avossa, A.M. Characterization of Mean Wind Profiles and Surface Roughness Assessment from Wind LIDAR Measurements. In Proceedings of the XV Conference of the Italian Association for Wind Engineering, IN VENTO 2018, Naples, Italy, 9–12 September 2018; Ricciardelli, F., Avossa, A., Eds.; Springer: Cham, Switzerland, 2019; Volume 27, pp. 689–702.
20. Cook, N.J. The Deaves and Harris ABL model applied to heterogeneous terrain. *J. Wind Eng. Ind. Aerodyn.* **1997**, *66*, 197–214. [CrossRef]
21. Tieleman, H.W. Strong wind observations in the atmospheric surface layer. *J. Wind Eng. Ind. Aerodyn.* **2008**, *96*, 41–77. [CrossRef]
22. Li, Q.; Zhi, L.; Hu, F. Boundary layer wind structure from observations on a 325 m tower. *J. Wind Eng. Ind. Aerodyn.* **2010**, *98*, 818–832. [CrossRef]
23. Högström, U. Review of some basic characteristics of the atmospheric surface layer. *Bound.-Layer Meteorol.* **1996**, *78*, 215–246. [CrossRef]
24. WMO. *Guide to Meteorological Instruments and Methods of Observation, (WMO-No. 8) Volume III Observing Systems*; World Meteorological Organization: Geneva, Switzerland, 2021.
25. Wieringa, J. Does representative wind information exist? *J. Wind Eng. Ind. Aerodyn.* **1996**, *65*, 1–12. [CrossRef]
26. Lindelöw, P.; Courtney, M.; Parmentier, R.; Cariou, J.P. Wind shear proportional errors in the horizontal wind speed sensed by focused, range gated lidars. *IOP Conf. Ser. Earth Environ. Sci.* **2008**, *1*, 012023. [CrossRef]
27. Lindelöw-Marsden, P. *UpWind D1. Uncertainties in Wind Assessment with LIDAR*; Technical Report, Risø-R-1681(EN); Risø National Laboratory (Den.); Technical University of Denmark: Roskilde, Denmark, 2009.